Unified description of stimulated-Raman-scattering and four-wave mixing in wavelength-division-multiplexed systems

Frédérique Vanholsbeeck, G. Van Simaeys, Philippe Emplit, *Member*, IEEE,
Marc Haelterman, and Thibaut Sylvestre

Service d'Optique et d'Acoustique, Université Libre de Bruxelles,
CP 194/5, Avenue F.D. Roosevelt 50, B-1050 Brussels, Belgium.

A detailed theoretical analysis is presented that illustrates the crosstalk induced simultaneously by stimulated-Raman-scattering and four-wave mixing in wavelength-division multiplexed systems. This analysis is based on numerical simulations of coupled-mode equations that allow to predict accurately the Raman-induced spectral power tilt for unlimited optical bandwidth. By means of a realistic example, we show that this power tilt can be drastically reduced in a distributed dual-pump Raman amplification scheme. It is also shown that multiple four-wave mixing interactions induce strong parametric oscillations whose dynamics is essentially ruled by the channel spacing and the group-velocity dispersion.

Introduction

Third-order nonlinear effects such as stimulated Raman scattering (SRS) and four-wave mixing (FWM) limit the performance of wavelength-division-multiplexed (WDM) transmission systems [1]. On one hand, SRS induces power transfer from lower to higher wavelength channels resulting in a tilt in the power distribution among channels. On the other hand, for small channel spacings, four-wave mixing leads to the generation of undesirable parametric sidebands that can interfere with system operation [2]. Though these two effects have been thoroughly investigated, they have never been studied simultaneously in WDM systems. Moreover, SRS has only to date been considered through a triangular approximation of the Raman gain curve [3, 4, 5].

In this letter, we present a coupled-mode theory that fully describes the dynamics of equally-spaced WDM channels interacting through Kerr and Raman effects simultaneously. In order to get a realistic insight into the involved phenomena, we model the Raman response with the measured Raman gain curve of silica fibers [6]. We also take into account the dispersion and the attenuation of the fiber, as well as the self-and cross-phase modulations. In addition, we perform the simulations at 1.55μm for different channel spacings $\Delta\lambda$, initial mean powers $P_m(0)$, dispersion regimes and propagation lengths. On the basis of our theory, we propose a new simple scheme to compensate the Raman-induced power tilt between the channels.

Characterization and compensation of the Raman-induced power tilt

Let us first study the Raman-induced power tilt for various channel spacings in an unamplified link. Studies based on the linear approximation of the Raman gain curve, suggest that the tilt grows exponentially as the channel spacing as far as the total WDM bandwidth is smaller than the Raman shift ($\Omega_R/2\pi$ = 13.2THz) [3, 4]. Figure 1(a) represents the power evolution for 6 WDM channels propagating through a 10km-long single-mode

fiber (SMF). It clearly shows that the power of all channels decreases due to the fiber loss. The difference of loss between each WDM channel result from the SRS-induced power transfers, which causes the tilt in the output power spectrum distribution as can be viewed in the inset of Fig. 1(a). From a Lorentzian approximation of the Raman response curve, we derive a general analytical formula for the power ratio $(P_1/P_N)_{dB}$ that reads as

$$(P_1/P_N)_{dB} = 4.34 \cdot P_m(0) \cdot 2g(\Omega_R)(\frac{\omega_l}{2})^2 \sum_{j=1}^{N-1} \frac{1}{((N-j)\Delta\omega - \Omega_R)^2 + (\frac{\omega_l}{2})^2} \cdot L_{\text{eff}} \qquad (1)$$

where $g(\Omega_R)$ is the maximum of the Raman gain curve, ω_l is its full width at half maximum (7.2THz), N is the number of channels, $\Delta\omega$ is the channel spacing, and $L_{eff} = (1-e^{\alpha z})/\alpha$ is the effective length that accounts for the loss. In Fig. 1(b), we plot the power ratio as a function of the total bandwidth (N-1)$\Delta\omega$ for the linear approximation of Ref. [4] (dotted line), for our analytical Lorentzian approximation (solid line) as well as for our simulation results (dashed-dotted line). Compared with the usual triangular approximation, these two last curves clearly demonstrate that the detrimental impact of SRS strongly decrease for a total bandwidth slightly greater than the Raman shift.

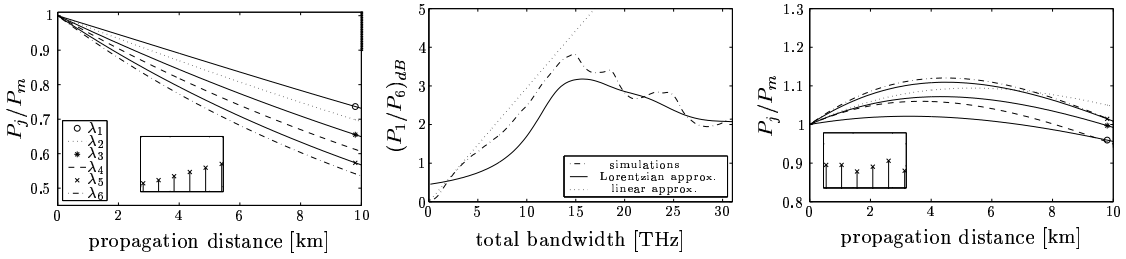

(a) Normalized power evolution of 6 WDM channels at 1.55μm, D = 16.7ps/nm/km, L = 10km, P_t = 48mW (17dBm) and $\Delta\lambda$ = 8nm. The insets show the output spectral power distribution at 10km. $(P_1/P_6)_{dB}$ = 1.36dB, $\Delta P = 47 \times 10^{-4}$.

(b) Power ratio (dashed-dotted line) as a function of the total bandwidth. The dotted and the solid lines are, respectively, the triangular and the Lorentzian approximations for the power ratio.

(c) Normalized power evolution of the same WDM system as Fig.1(a) with two pumps: $\lambda_{P_1} = 1422nm, \lambda_{P_2} = 1448nm, P_{P_1} = 28.8mW$ and $P_{P_2} = 24mW$. The inset shows the output spectrum. $(P_1/P_6)_{dB}$ = 0.23dB, $\Delta P = 11 \times 10^{-4}$.

Figure 1: Characterization and compensation of the Raman-induced power tilt.

As the Raman-induced tilt is one of the major limitations of transmission performances, its suppression would allow for increased total bandwidth, power per channel and amplifier spacing along the transmission line [7]. We suggest to exploit the particular shape of the Raman gain curve to compensate the tilt through a forward dual-pumped Raman amplification scheme. With a proper choice of the pump wavelengths, the SRS-induced tilt could be balanced by the resulting gain curve. The lower-wavelength pump amplifies the lower-wavelength channels while the second pump power is transferred to the middle channels. As a result, the upper-wavelength channels, which fall outside the pumps bandwidth, get essentially amplified through the SRS from the lower-wavelength channels. This principle of Raman tilt suppression is illustrated in Fig. 1(c) that shows the same power evolution as in Fig. 1(a) but now in the presence of two pumps at 1422nm

and 1448nm respectively. For the convenience of the analysis, we introduced the standard deviation of the total power $\Delta P = \sum_{j=1}^{N}((P_j(L) - P_m(L))^2)/P_m^2(0))$. With our Raman compensating technique, the tilt is reduced by 83% and the power deviation ΔP by 77%. As we can see in Fig. 1(c), the forward pumping scheme presents however some important drawbacks for longer amplifier spacing. Indeed, the pump waves are completely depleted before the output of the fiber while the SRS-induced transfer goes on all over the fiber span, leading to an asymmetry in the power distribution between the WDM channels. Increasing the initial pump power does not make sense as pumps depletion would happen faster. We expect that this difficulty can be alleviated in a backward pumping configuration. We believe that this two-pump Raman amplification technique for achieving Raman-induced power tilt suppression constitutes a simple and promising solution that could be implemented in future telecommunication systems.

Influence of the four-wave mixing

To complete this study, we also investigated the power exchanges induced by FWM between channels in WDM systems in the presence of SRS. The amplitude of the FWM products increases as the minimum linear phase mismatch ($\Delta k = \beta_2 \Delta\omega^2$) decreases. Therefore, we consider a channel spacing as low as 1nm corresponding to a total frequency bandwidth of 0.6THz, which is much smaller than the Raman shift. In this configuration, SRS effect remains small in comparison with the FWM processes.

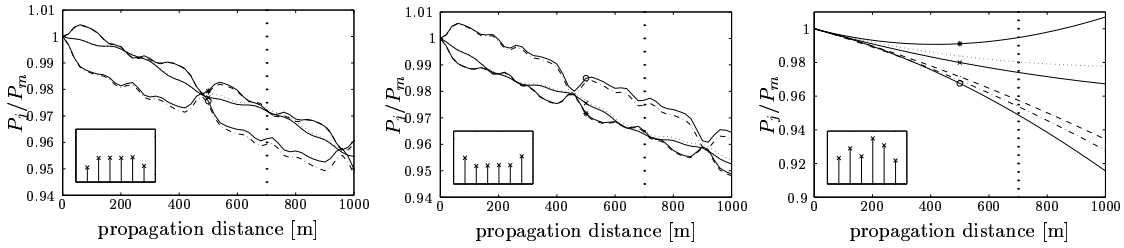

(a) D=16.7ps/nm/km. (b) D=-17.6ps/nm.km. (c) D=1.17ps/nm.km.

Figure 2: Normalized power evolution of 6 WDM channels at 1.55μm, L = 1km, P_m = 8mW, $\Delta\lambda$ = 1nm in different dispersion regimes. The dotted lines indicate where the spectral power distributions shown in the insets are measured.

The simulations whose results are shown in Fig. 2(a) and 2(b) and performed, respectively, in the anomalous and normal dispersion regime. The power exchanges exhibit a recurrent dynamics over a large fiber length that corresponds to the maximum coherence length ($L_c = 2\pi/\Delta k$) associated with the most efficient FWM processes. As a result, the power tends to concentrate in the central channels in the anomalous dispersion regime whereas the opposite behavior is observed in the normal dispersion regime as shown in the insets. In Fig. 2(c) are depicted the results obtained in the nearly zero-dispersion regime. In this case, the power exchanges are no longer recurrent because the FWM processes are nearly phase-matched giving rise to strong parametric power transfers ($L_c \to \infty$ as $\Delta k \to 0$). It is worth noting that the dynamics are entirely determined once the dispersion regime and the initial phases of the channels are fixed.
In Fig. 3(a) that differs from Fig.2(a) only by the initial phase mismatches between channels, i.e. the anomalous dispersion parameter is D = 16.7ps/nm.km, we can observe that

the amplitude of parametric oscillations increases. These results suggest that, by a proper control of initial phases and dispersion regime, it should be possible to reduce the amplitude of the FWM processes. In Fig. 3(b) and Fig. 3(c), we show the resulting output power spectra for a channel spacing of 1.5 and 2nm respectively. With such channel spacings we emphasize the mutual influence of SRS and FWM. As can be seen in Fig. 3(c), the tilt due to SRS is periodically compensated by the FWM process for anomalous dispersion ($\Delta P = 2.6 \times 10^{-6}$ at 600 m and 6.2×10^{-6} at 700 m).

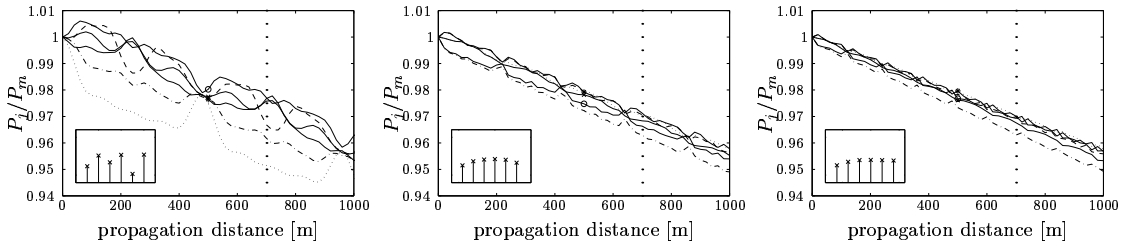

(a) $\Delta\lambda$ = 1nm. (b) $\Delta\lambda$ = 1.5nm. (c) $\Delta\lambda$ = 2nm.

Figure 3: Normalized power evolution of 6 WDM channels at 1.55μm, L = 1km, P_m = 8mW in a SMF for different channel spacings. For (a), the channels are mismatched at the input of the fiber. The dotted lines indicate where the spectral power distributions shown in the insets are measured.

Conclusion

By introducing the measured Raman gain curve in our model we have shown that the impact of SRS-induced impairment in WDM systems dramatically decreases with respect to the triangular approximation. We have also demonstrated that two-pump distributed Raman amplification can be exploited to control and reduce the Raman-induced power tilt. Moreover, we have characterized the periodic power exchanges between channels due to four-wave mixing and its influence on the Raman-induced power tilt.

References

[1] A. R. Chraplyvy. Limitations on lightwave communications imposed by optical-fiber nonlinearities. *IEEE J. Lightwave Technol.*, 8(10):1548–1557, October 1990.

[2] R. W. Tkach, A. R. Chraplyvy, F. Forghieri, A. H. Gnauck, and R. M. Derosier. Four-photon mixing and high-speed WDM systems. *IEEE J. Lightwave Technol.*, 13(5):841–849, May 1995.

[3] D. N. Christodoulides and R. B. Jander. Evolution of stimulated Raman crosstalk in wavelength division multiplexed systems. *IEEE Photon. Technol. Lett.*, 8(12):1722–1724, December 1996.

[4] S. Bigo, S. Gauchard, A. Bertaina, and J. P. Hamaide. Experimental investigation of stimulated Raman scattering limitation on WDM transmission over various types of fiber infrastructures. *IEEE Photon. Technol. Lett.*, 11(6):671–673, June 1999.

[5] A. G. Grandpierre, D. N. Christodoulides, and J. Toulouse. Theory of stimulated Raman scattering cancellation in wavelength-division-multiplexing systems via spectral inversion. *IEEE Photon. Technol. Lett.*, 11(10):1271–1273, October 1999.

[6] R. W. Hellwarth. Third-order optical susceptibilities of liquids and solids. *Prog. Quantum Electron.*, 5(1–A):1–68, 1977.

[7] H. S. Seo, W. Shin, U. C. Ryu, and U. C. Paek. Compensation of Raman-induced crosstalk using a lumped germanosilicate fiber Raman amplifier in the 1.571-1.591-μm region. *IEEE Photon. Technol. Lett.*, 13(1):28–30, January 2001.